Desalination and Water Treatment
www.deswater.com

doi: 10.5004/dwt.2017.0080

60 (2017) 228–241
January

Determination of design parameters for the cloud point extraction of Remazol Turquoise Blue G-133 dye using Triton X-114 surfactant

Dhanabalan Duraimurugan alias Saravanan[a], Thanabalan Murugesan[b], Appusamy Arunagiri[a,*]

[a]*Department of Chemical Engineering, National Institute of Technology, Tiruchirappalli 620015, Tamilnadu, India, Tel. +91-431-2503114; Fax: +91-431-2500133; emails: aagiri@nitt.edu (A. Arunagiri), duraisaran31@gmail.com (D. Duraimurugan alias Saravanan)*
[b]*Chemical Engineering Department, Universiti Teknologi Petronas, 31750 Tronoh, Perak, Malaysia, email: murugesan@petronas.com.my*

Received 21 January 2016; Accepted 20 May 2016

ABSTRACT

A design method has been proposed for cloud point extraction (CPE) process. The aim was to determine the concentration of non-ionic surfactant Triton X-114 (TX-114) needed to achieve the preferred extraction of Remazol Turquoise Blue G-133 (RTB G-133) dye at different operating conditions (feed dye concentration and temperature). The solute concentrations of 25, 50, and 75 ppm, and surfactant concentrations of about 0.01–0.1 M were used. The feasibility of the CPE process was also studied using the thermodynamic parameters. For design calculations, knowledge of the following two features were needed: (1) the solubilization isotherm of RTB G-133 in TX-114 at different operating temperatures and (2) estimation of the change of the fractional coacervate phase volume with the feed surfactant, dye concentration and the operating temperature. The experimental data were fitted on to a Langmuir type solubilization isotherm. Correlations were then established for the variation of isotherm parameters with temperature. From the defined correlations and formulated design method, the concentration of feed surfactant necessary to obtain 1 ppm concentration of dye in the dilute phase was evaluated at specific operating temperatures and feed dye concentrations. The design method developed will greatly aid the scale-up of CPE.

Keywords: Remazol Turquoise Blue G-133; Triton X-114; Cloud point extraction; Isotherm; Fractional coacervate

1. Introduction

Man-made dyes and pigments are added to the environment through effluents from textile, leather, paper, plastic, and printing industries [1]. The colored compounds tend to persist in the environment, decline the water quality and lead to allergies, skin irritation, cancer and mutation [2]. These compounds also obstruct the absorption of solar rays and alter the photosynthetic activity causing severe decline in the aquatic biodiversity [3]. Reactive dyes are produced in a large scale than any other class of dyes and are favored by the consumer for their bright colors and high wet fastness [4]. Reactive dye belongs to the class copper phthalocyanine with a reactive group of sulphatoethylsulphone. Copper phthalocyanine dyes are widely used in textile industry and resist bacterial degradation [3]. Remazol Turquoise Blue-G 133 (RTB G-133) is one such reactive dye based on copper phthalocyanine and is highly preferred owing to its chemical stability, brilliant blue color, and high tinctorial strength. RTB G-133 comprises tetra sulfonated copper phthalocyanine with one to two of the sulfonate groups transformed to linker arms [5]. Reactive dyes are also the most problematic compounds in wastewaters from textile industries owing to their high solubility in water and need to be treated before disposal to improve the

* Corresponding author.

quality of water [6]. Several techniques are available for the removal of color from wastewater including nanofiltration [7], adsorption onto different substances such as agricultural solid waste [8], micellar-enhanced ultrafiltration [9], different bentonites [10], ozonations [11], several oxidation processes [12,13], various types of activated carbon [14], surfactant impregnated montmorillonite [15] and so on. However, each method has its own limitations. Due to low biodegradability of dyes, colored effluents cannot be removed efficiently by a conventional biological wastewater treatment process [16].

In the last decade, the potential of aqueous micellar solution in the field of separation science is clearly identified [17]. A novel technology for effluent treatment involves surfactant-based separation methods. Cloud point extraction (CPE) is one such method used for removing dye from aqueous solutions. At certain temperature (i.e., cloud point, CP), aqueous solution of a nonionic surfactant becomes turbid. The further increase in temperature (above the CP) separates the solution into two different phases: a surfactant rich phase (also known as coacervate phase) and a dilute phase containing surfactant concentration slightly above the critical micelle concentration (CMC) [18–28]. A number of authors have investigated the mechanisms for phase separation of non-ionic surfactants above CP [20–23]. The phase separation occurs due to the dehydration of exterior layer of micelles of non-ionic surfactant, intermicellar attractive force, and increase in micellar size [24]. The solubilization of dye occurs in the mantle and the core of the micelles, based on its polarity. The non-polar solubilizates and polar solubilizates are solubilized in the core of micelles and in the mantle, owing to the increase in the aggregation of micelles and the dehydration of the polyoxyethylene chains, respectively [19,29,30]. The physical properties of heterogeneous phases of aqueous micellar solution provide information about the molecular interactions in the mixture. The density, viscosity, and refractive index are essential to understand the thermodynamic behaviors of solute or solvent in liquid mixtures [22].

In the present work, CPE of RTB G-133 dye from wastewater, using Triton X-114 (TX-114) as a non-ionic surfactant has been studied. The CPEs were carried out for different combinations of varying concentrations of TX-114 and RTB G-133. The physical properties such as density, viscosity, and refractive index for the surfactant dilute phase and the surfactant rich phase were determined at 40°C, 50°C, and 60°C. The effects of various design parameters, such as surfactant concentration, dye concentration, and CP temperature (CPT) on phase-volume ratio and extraction efficiency, were investigated at different temperatures. Thermodynamic parameters, such as change in enthalpy ($\Delta H°$), change in entropy ($\Delta S°$), and Gibbs free energy ($\Delta G°$), were determined at different temperatures, and the feasibility of CPE using TX-114 for the removal of dyes from aqueous solution was confirmed.

2. Materials

RTB G-133 dye (Formula Weight (FW): 576.10, λ_{max}: 624 nm, dye content: 97%, product of USA), and TX-114 (t-Octylphenoxy polyoxyethylene ether, with approximately 8,9-ethoxy units per molecule [density at 25°C is 1.058 g. m1^{-1}, Molecular Weight (Mol. Wt.): 537, λ_{max}: 223 nm, purity: 95%, product of USA]) were purchased from Sigma-Aldrich, India. The critical micellar concentration (CMC) of TX-114 is 2.1×10^{-4} M at 25°C, and the CPT is 23°C. RTB G-133 dye was used as solute; TX-114 was used as the non-ionic surfactant as shown in Figs. 1 and 2, respectively.

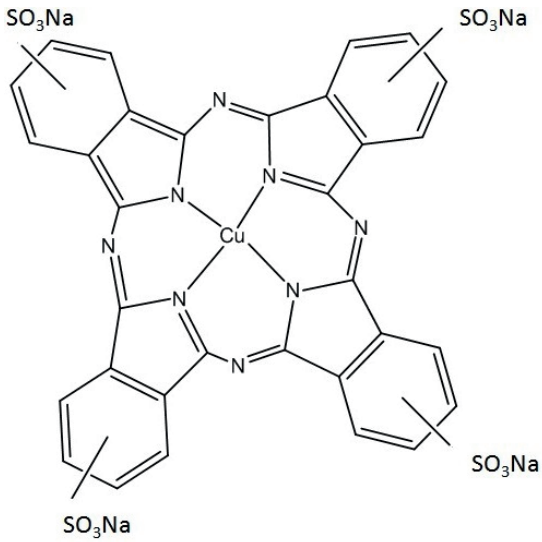

Fig. 1. Molecular structure of RTBG-133.

JASCO UV-visible spectrophotometer was used for calibration and measuring the dye concentration in dilute phase after phase separation. The densities of surfactant dilute phase and surfactant rich phase were determined using specific gravity bottle (5 ml) and weighing balance (Sartorius, Germany) with a precision of ±0.1 mg. The uncertainty of the measured density was ±0.0001. BROOKFIELD (DV-II + PRO) viscometer was used to measure the viscosity of the solutions. The uncertainty in the viscosity measurements was found to be ±1.0%. The refractive indices of the surfactant dilute and surfactant rich phases were measured using abbe refractometer (Guru Nanak Instruments, New Delhi) with a precision of ±0.0005. Water bath (Technico Laboratory Products, Chennai) was used to maintain the desired temperature for CPE. The temperatures were maintained with an accuracy of ±0.2°C.

3. Methods

3.1. Solution preparation

Aqueous micellar solutions of 50 ml were prepared with various concentrations of solute and surfactant. Different concentrations of dye solutions were prepared and used to calibrate the UV-visible spectrophotometer. Solute concentration was varied from 25 to 75 ppm, respectively, and the surfactant concentration ranged from 0.01 to 0.1 M. Solutions were heated above CPT till separation of phases occurred. The concentrations of solute were 25, 50, and 75 ppm, while the surfactant concentration was varied from 0.01 to 0.1 M [6].

3.2. Determination of CPT

The temperature at which the micellar solution becomes turbid is visually observed and is referred to as a CPT. The turbidity appears due to the scattering of visible light by the large

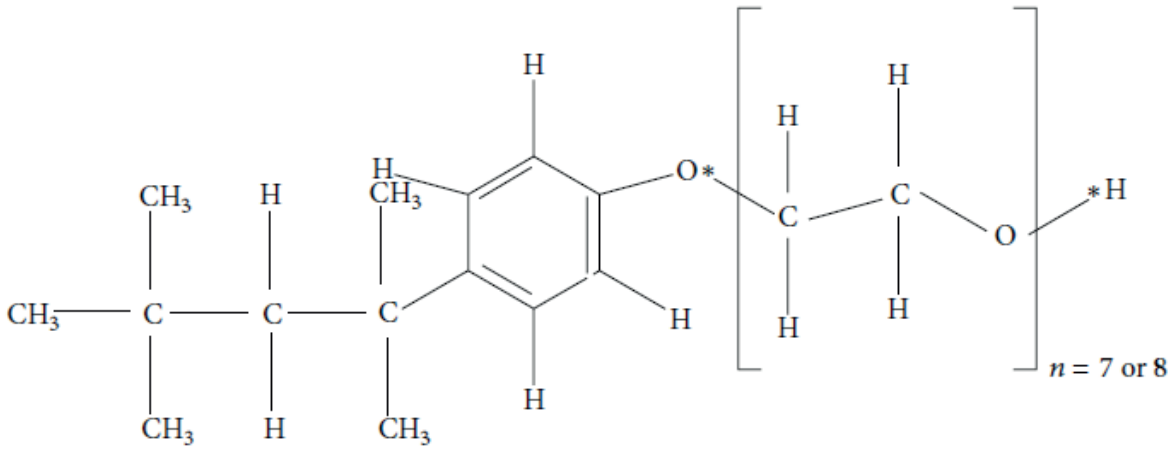

Fig. 2. Chemical structure of Triton X-114.

surfactant aggregates known as micelles. The CP of the prepared aqueous non-ionic surfactant solution was determined by heating it in a thermostatic water bath, and the temperature was increased at a rate of 1°C per min. The temperature at which the micellar solution became turbid was noted as the CPT. On heating the turbid solution above the CPT, the solution got separated into two different phases, namely a surfactant rich phase and a surfactant dilute phase. The surfactant rich phase is enriched in surfactant aggregates (micelles), whereas the surfactant dilute phase is depleted of such surfactant micelles. This process is reversible, and these heterogeneous mixtures become homogeneous when cooled below the CPT. The experiments were performed for different combinations of surfactant and solute concentrations. All the CPTs reported were the average of triplicate measurements with an accuracy of ±0.2°C. The CPTs were found to vary in the range of 40°C–60°C. Based on these measurements, the operating temperatures were selected.

3.3. CPE of RTB G-133 dye

Aqueous micellar solutions were prepared, respectively, with varying concentrations of dye (25, 50 and 75 ppm) and TX-114 (0.01–0.1 M). The samples were kept in the thermostatic bath maintained at the desired temperatures (40°C, 50°C, and 60°C, respectively) based on the CPT for 30 min. After the formation of heterogeneous clear phases, the volumes of surfactant rich phase and dilute phase were noted down. Then, the concentrations of RTB G-133 in dilute phases were determined by UV-visible spectrophotometer, and subsequently, the concentrations of dye in surfactant rich phases were obtained using material balance. Physical properties such as density and refractive index were measured for both the surfactant dilute and rich phases. Phase volume ratio and extraction efficiency were analyzed. Thermodynamic properties such as change in enthalpy ($\Delta H°$), entropy ($\Delta S°$) and Gibbs free energy ($\Delta G°$) were also evaluated.

4. Results and discussion

In CEP, the phenomenon of formation of two incompatible phases above CPT is used for the solubilization of the dyes. The phase separation begins as a consequence of either miscibility of micelles or the separation of micelles from water. The physical property of the two phases also aids the phase separation. The density difference between the surfactant rich phase and surfactant dilute phase results in such physical separation of two different phases [31,32]. The physical properties such as density, refractive index, and viscosity are necessary to be acquainted with the thermodynamic behavior of solute or solvent in liquid mixtures [22].

4.1. Effects of surfactant, solute concentration, and temperature on physical properties of dilute and surfactant rich phases

The effects of surfactant and solute concentration on the density, refractive index, and viscosities of dilute and surfactant rich phases are provided in Tables 1–3.The surfactant rich phase consisted of surfactant, dye, and water molecules. The number of micelles and the size of the micelles increased with the increase in surfactant concentration [33]. As a result, the surfactant settled into the surfactant rich phase, and the density difference between the two phases increased. Again with large number of micelles, more amount of dye solute was solubilized with surfactant micelles in the surfactant rich phase. Hence, the density increased with the increase in the surfactant concentration. The increase in temperature resulted in an increased solubility of the dye. At higher temperatures, the water molecules escaped from the external layers of the micelle resulting in the decrease of water content and making the solution very dense.

The refractive index of dilute phase was found to be almost nearer to that of refractive index of water (1.332) at all concentrations of surfactant. This ensures that the dilute phase obtained after the CPE was similar to that of water. The increase in the solute concentration had increased the density, decreased the speed of light through the medium, thereby increasing the refractive index of the medium. Hence, the refractive index of the surfactant rich phase increased with the surfactant concentration, and that of the dilute phase was nearly constant similar to water.

Table 1
Physical properties for 75 ppm of surfactant dilute phase and surfactant rich phase at 313.15, 323.15 and 333.15 K

TX-114 (M)	Density (g cm^{-3})	Refractive index	Viscosity (mPa s)	Density (g cm^{-3})	Refractive index	Viscosity (mPa s)
Surfactant dilute phase at 313.15 K				Surfactant rich phase at 313.15 K		
0.02	0.998	1.331	0.86	1.022	1.361	NA
0.04	0.998	1.332	0.88	1.025	1.361	NA
0.06	0.997	1.332	0.9	1.027	1.362	157.3
0.08	0.996	1.334	0.88	1.028	1.368	179.6
0.1	0.994	1.332	0.9	1.029	1.372	195.8
Surfactant dilute phase at 323.15 K				Surfactant rich phase at 323.15 K		
0.02	1.034	1.332	1.00	1.025	1.364	NA
0.04	1.033	1.333	0.99	1.028	1.364	NA
0.06	1.032	1.332	0.99	1.030	1.366	160.7
0.08	1.031	1.332	0.98	1.032	1.371	188.4
0.1	1.03	1.332	0.98	1.033	1.371	201.2
Surfactant dilute phase at 333.15 K				Surfactant rich phase at 333.15 K		
0.02	1.035	1.33	1.00	1.033	1.362	NA
0.04	1.034	1.332	0.99	1.034	1.361	NA
0.06	1.034	1.331	0.99	1.036	1.364	169.5
0.08	1.033	1.331	0.99	1.037	1.365	190.3
0.1	1.032	1.332	0.99	1.038	1.366	208.6

Table 2
Physical properties for 50 ppm of surfactant dilute phase and surfactant rich phase at 313.15, 323.15 and 333.15 K

TX-114 (M)	Density (g cm^{-3})	Refractive index	Viscosity (mPa s)	Density (g cm^{-3})	Refractive index	Viscosity (mPa s)
Surfactant dilute phase at 313.15 K				Surfactant rich phase at 313.15 K		
0.02	0.998	1.333	1.00	1.023	1.362	NA
0.04	0.996	1.333	0.97	1.024	1.630	NA
0.06	0.995	1.333	0.96	1.025	1.364	145.6
0.08	0.994	1.332	0.96	1.026	1.365	174.1
0.1	0.994	1.332	0.96	1.027	1.371	189.9
Surfactant dilute phase at 323.15 K				Surfactant rich phase at 323.15 K		
0.02	1.033	1.332	0.99	1.024	1.364	NA
0.04	1.032	1.332	0.99	1.025	1.364	NA
0.06	1.031	1.332	0.99	1.026	1.365	153.1
0.08	1.030	1.333	0.98	1.031	1.368	179.3
0.1	1.029	1.333	0.97	1.032	1.371	191.7
Surfactant dilute phase at 333.15 K				Surfactant rich phase at 333.15 K		
0.02	1.035	1.332	0.99	1.032	1.362	NA
0.04	1.034	1.332	0.98	1.034	1.361	NA
0.06	1.033	1.332	0.98	1.035	1.366	162.4
0.08	1.032	1.332	0.98	1.036	1.366	183.9
0.1	1.031	1.333	0.98	1.036	1.368	196.5

The viscosity of TX-114 surfactant is relatively high (260 cp at 25°C), when compared with that of water (0.894 cp at 25°C). The viscosity of the mixture strongly depended on the presence of water. When the surfactant concentration was increased, the surfactant rich phase became more viscous compared with the dilute phase owing to the molecular attraction between identical structures of the molecules. The increase in the temperature resulted in an increase in the viscosity of surfactant rich phase due to the removal of water molecules from the external layers of micelles. On contrary, at higher temperature,

Table 3
Physical properties for 25 ppm of surfactant dilute phase and surfactant rich phase at 313.15, 323.15 and 333.15 K

TX-114 (M)	Density (g cm^{-3})	Refractive index	Viscosity (mPa s)	Density (g cm^{-3})	Refractive index	Viscosity (mPa s)
Surfactant dilute phase at 313.15 K				Surfactant rich phase at 313.15 K		
0.02	0.998	1.333	0.89	1.017	1.358	NA
0.04	0.995	1.333	0.90	1.017	1.359	NA
0.06	0.995	1.332	0.88	1.017	1.361	136.2
0.08	0.993	1.332	0.88	1.019	1.362	149.6
0.1	0.991	1.331	0.86	1.021	1.363	145.2
Surfactant dilute phase at 323.15 K				Surfactant rich phase at 323.15 K		
0.02	1.037	1.331	0.87	1.022	1.358	NA
0.04	1.034	1.332	0.88	1.027	1.359	NA
0.06	1.028	1.331	0.87	1.030	1.360	147.1
0.08	1.027	1.331	0.87	1.035	1.362	159.5
0.1	1.025	1.333	0.90	1.038	1.363	171.3
Surfactant dilute phase at 333.15 K				Surfactant rich phase at 333.15 K		
0.02	1.039	1.332	0.88	1.031	1.356	NA
0.04	1.031	1.331	0.87	1.033	1.360	NA
0.06	1.029	1.332	0.88	1.034	1.362	159.7
0.08	1.024	1.332	0.88	1.035	1.363	173.8
0.1	1.022	1.333	0.89	1.036	1.365	192.1

the dilute phase viscosity decreased with the addition of water molecules due to the weak hydrogen bond interactions and had reached a constant value. Arunagiri et al. [33] reported the experimental data for the separation of methylene blue dye using CPE and observed the similar trend for the variations of density, refractive index, and viscosity.

4.2. Effect of surfactant, solute concentration, and temperature on phase volume ratio

The phase volume ratio (R_V) is defined as the ratio of the volume of the surfactant-rich phase to that of the aqueous phase and is determined using the following formula:

$$R_V = V_s / V_w \quad (1)$$

where V_s and V_w are the volumes of the surfactant-rich phase and the aqueous phase, respectively.

The phase volume ratio increased with increase in surfactant (TX-114) concentration and solute (RTB G-133) concentration and is shown in Figs. 3(a)–(c). For instance, Fig. 3(a) shows that at a constant temperature of 60°C and a surfactant concentration of 0.1 M, the phase volume ratio increased from 29.87 to 46.19 for an increase in dye concentration from 25 to 75 ppm. Similarly, for a constant temperature of 60°C and a lower surfactant concentration of 0.01 M, the phase volume ratio increased from 2.45 to 5.93 for an increase in dye concentration from 25 to 75 ppm. The increase in surfactant concentration resulted in increase in phase volume ratio owing to the increase in the volume of coacervate phase. Hence, at higher surfactant concentration, the additional amount of surfactant entered the coacervate phase (surfactant rich phase) and had maintained the material balance as the concentration of surfactant remained constant and near CMC in the dilute phase [9,25]. However, for a constant dye concentration, the phase volume ratio decreased with the increase in temperature. The effect of operating temperature on the phase volume ratio at a constant dye concentration is shown in Figs. 4(a)–(c). As the temperature increased, interaction among micelles of TX-114 would be predominant, and dehydration took place from external layers of micelles. This resulted in reduction in the volume of coacervate phase. Hence, the phase volume ratio decreased with increase in operating temperature [33].

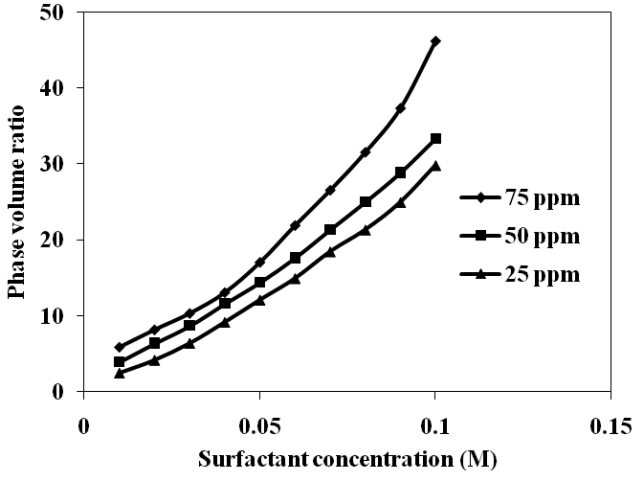

Fig. 3(a). Effect of concentrations of surfactant and solute on phase volume ratio at 60°C.

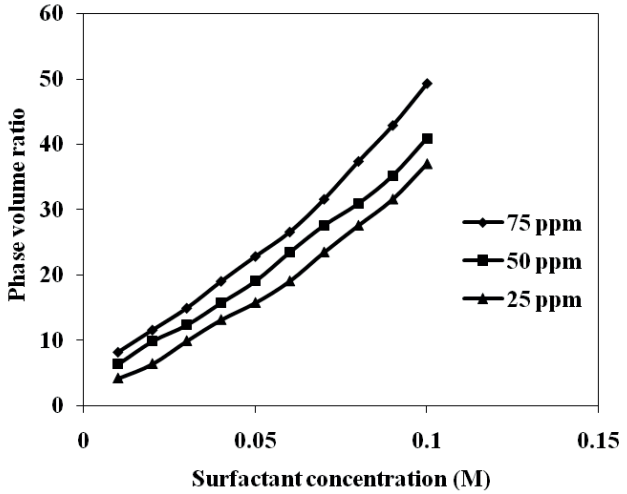

Fig. 3(b). Effect of concentrations of surfactant and solute on phase volume ratio at 50°C.

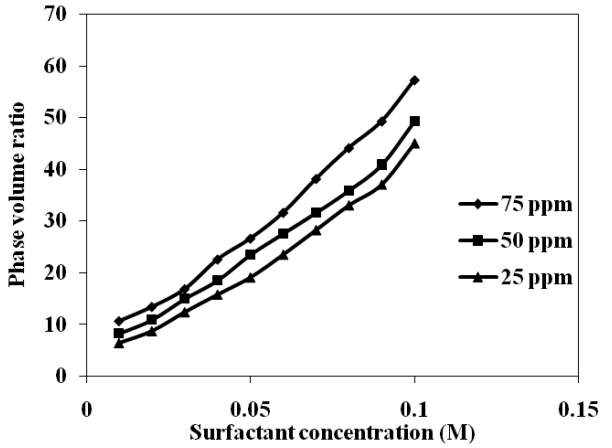

Fig. 3(c). Effect of concentrations of surfactant and solute on phase volume ratio at 40°C.

4.3. Effect of surfactant and solute concentrations and operating temperature on extraction efficiency (%)

The recovery or extraction efficiency of solute can be calculated as the percentage of solute extracted from the bulk solution into the surfactant-rich phase. It is calculated using the following expression.

$$\eta\% = \frac{C_o Vt - Cw(Vt - Vs)}{C_o Vt} * 100 \quad (2)$$

At a constant temperature and dye concentration, the extraction efficiency of dye increased with the feed surfactant concentration and is shown is Figs. 5(a)–(c). An extraction efficiency of 98.49% was obtained for 25 ppm solute concentration and at 60°C. The concentration of the micelles increased with the increase in feed surfactant concentration,

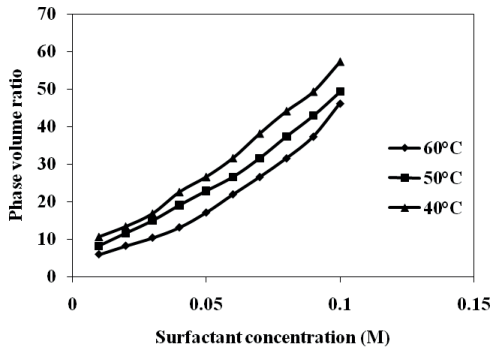

Fig. 4(a). Effect of operating temperature on the phase volume ratio at 75 ppm dye.

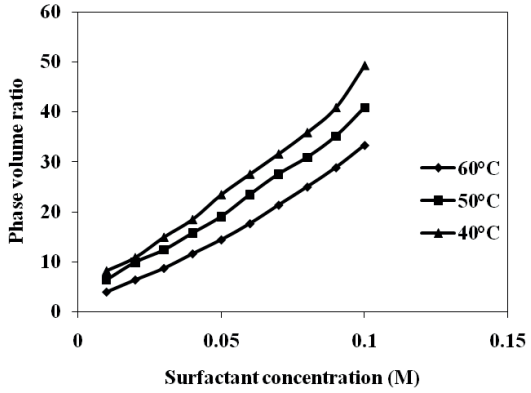

Fig. 4(b). Effect of operating temperature on the phase volume ratio at 50 ppm dye.

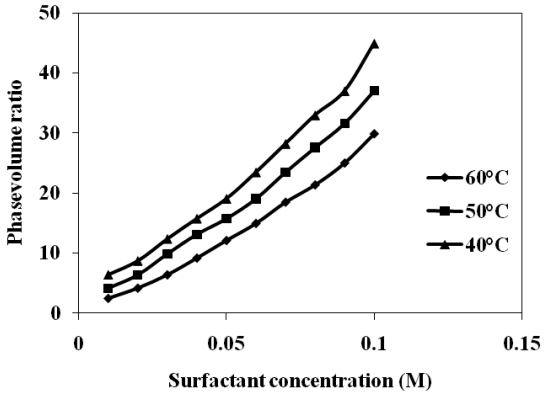

Fig. 4(c). Effect of operating temperature on the phase volume ratio at 25 ppm dye.

resulting in more solubilization of dyes into the micelles present in the surfactant rich phase. Consequently, the surfactant concentration in the dilute phase remained around CMC [34]. The extraction efficiency of dye decreased with increase in solute concentration for a particular temperature and surfactant concentration. The added solute remained in

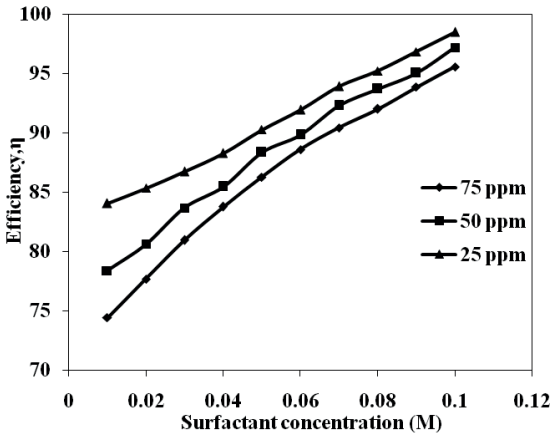

Fig. 5(a). Effect of surfactant and solute concentrations on efficiency (%) at 60°C.

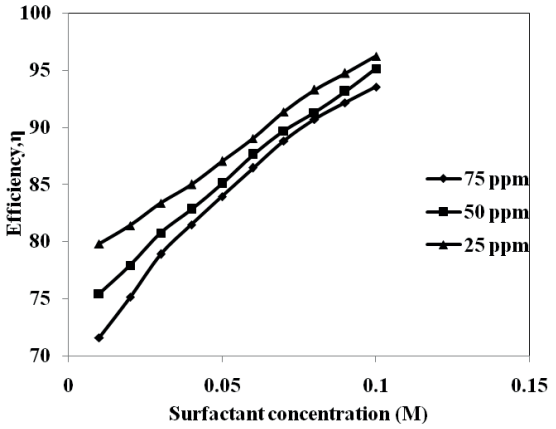

Fig. 5(b). Effect of surfactant and solute concentrations on efficiency (%) at 50°C.

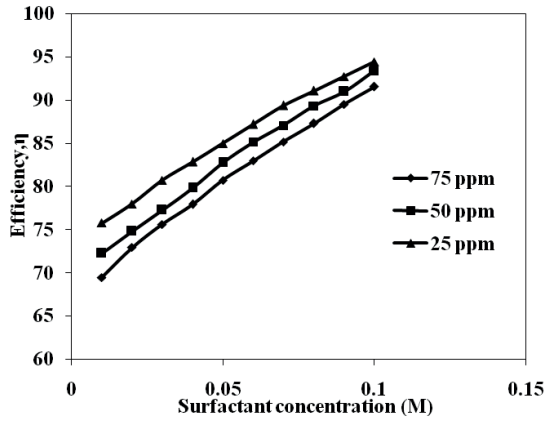

Fig. 5(c). Effect of surfactant and solute concentrations on efficiency (%) at 40°C.

the dilute phase at fixed surfactant concentration and operating temperature, decreasing the extraction efficiency of dye. The extraction efficiency increased with increase in temperature and is shown in Figs. 6(a)–(c). The extraction efficiency

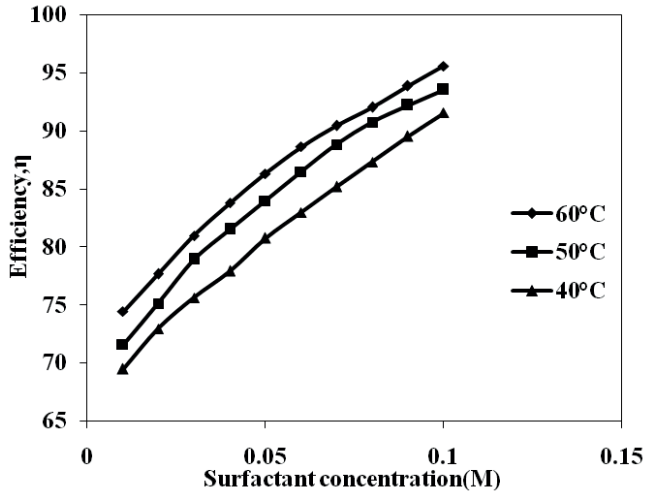

Fig. 6(a). Effect of operating temperature on efficiency (%) at 75 ppm.

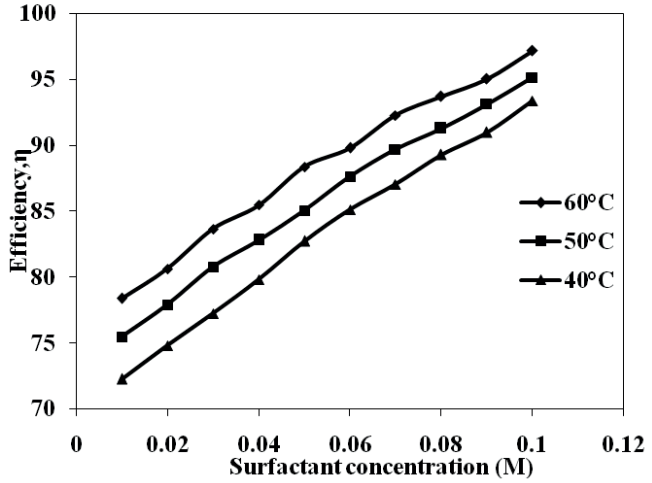

Fig. 6(b). Effect of operating temperature on efficiency (%) at 50 ppm.

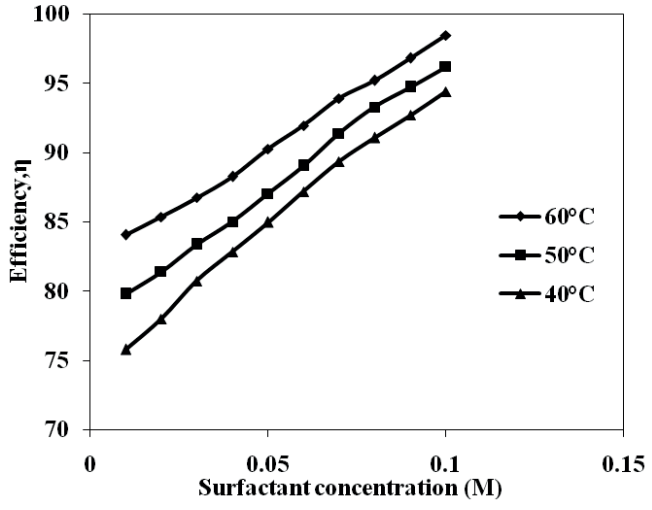

Fig. 6(c). Effect of operating temperature on efficiency (%) at 25 ppm.

of dye increased from 94.40% to 98.49% as the temperature varied from 40°C to 60°C for a surfactant concentration of 0.1 M and solute concentration of 25 ppm. The increase in temperature led to an increase in aggregation number and more micellar attraction, thereby increasing the solubilization of dye at higher temperatures. M.K. Purkait et al. studied the removal of dye using CPE technique and observed the similar trend [9,25].

4.4. Determination of thermodynamic parameters

Thermodynamic parameters are used to establish the possible mechanism for CPE of dyes and provide an idea about the feasibility of the process [35]. Different thermodynamic parameters, such as $\Delta G°$, $\Delta S°$ and $\Delta H°$, for the CPE of RTB G-133 dye were calculated using Eqs. (3)–(7) as follows:

$$\log\left[\frac{q_e}{C_e}\right] = \frac{\Delta S°}{2.303R} + \frac{-\Delta H°}{2.303RT} \tag{3}$$

$$\Delta G° = \Delta H° - T\Delta S° \tag{4}$$

where T is the temperature in Kelvin, q_e/C_e is called the solubilization affinity. q_e is the mole of dye solubilized per mole of non-ionic surfactant:

$$q_e = \frac{\text{Moles of dye solubilized}}{\text{Moles of TX}-100\text{ used}} = \frac{A}{X} \tag{5}$$

Moles of dye solubilized can be obtained from mass balance:

$$A = V_0C_0 - V_dC_e \tag{6}$$

$$X = C_sV_0 \tag{7}$$

where A is the mole of dye solubilized in the micelles. V_0 and V_d are the volume of the feed solution and that of the dilute phase after CPE, respectively. C_0 and C_s are the concentrations of surfactant in feed.

$\Delta S°$ and $\Delta H°$ can be obtained from a plot of log (q_e/C_e) vs. ($1/T$), from Eq. (3). Once these two parameters are obtained, $\Delta G°$ can be determined from Eq. (2).

4.5. Effects of solute and surfactant concentrations on the change of enthalpy ($\Delta H°$) of CPE

The variations in enthalpy change ($\Delta H°$) during CPE of RTB G-133 dye at different concentrations of TX-114–RTB G-133 dye are shown in Fig. 7. From Fig. 7, it is evident that the value of $\Delta H°$ increased with TX-114 concentration but decreased with the dye concentration. The positive values of $\Delta H°$ indicate that the solubilization of dye was endothermic in nature. For instance, at 25 ppm dye concentration, $\Delta H°$ value was 22,631.92 J mole^{-1} for 0.01 M surfactant concentration and increased to 58,264.75 J mole^{-1} for 0.1 M. The increase in $\Delta H°$ was due to the increase in the amount of dye solubilization with increase in surfactant concentration. Then, for a constant 0.1 M surfactant concentration, $\Delta H°$ decreased from 58,264.75 J mole^{-1} to 29,965.28 J mole^{-1} for 25 and 75 ppm, respectively. The decrease in $\Delta H°$ value with increasing dye concentration at a fixed surfactant concentration was due to the decrease in the amount of dye solubilization per mole of surfactant [30,36].

4.6. Effects of solute and surfactant concentrations on the change of entropy ($\Delta S°$) of CPE

The variations of entropy change ($\Delta S°$) during CPE of RTB G-133 dye at different concentrations of TX-114–RTB G-133 are shown in Fig. 8. The entropy changes were positive and indicated the good affinity of the dye molecules toward the surfactant micelles. It was found that the change in entropy ($\Delta S°$) increased with surfactant concentration but decreased with dye concentration for all the systems. Entropy depends on unsolubilized dye molecules and free surfactant molecules in the CPE system. For instance, at 25 ppm dye concentration, $\Delta S°$ value was 92.06 J mole^{-1}. K for 0.01 M surfactant concentration and increased to 200.09 J mole^{-1}.K for 0.1 M.

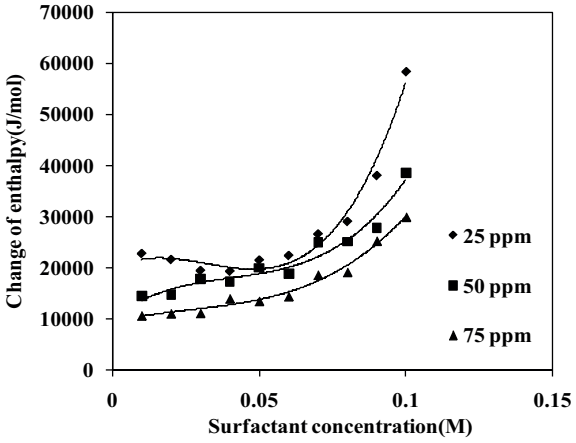

Fig. 7. Variation in Enthalpy change ($\Delta H°$) with TX-100 concentration.

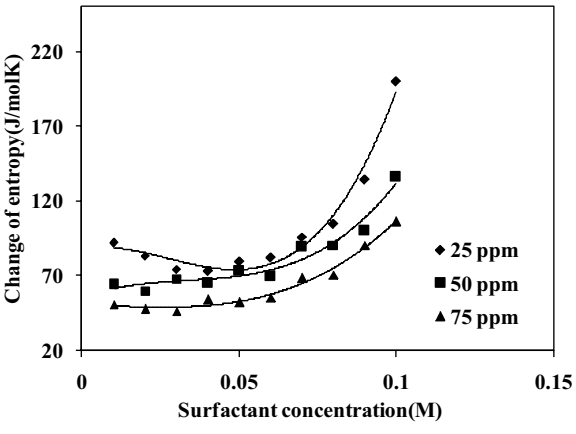

Fig. 8. Variation of Entropy change with TX-100 concentration.

The increase in $\Delta S°$ value with surfactant concentration was probably due to the increase of free surfactant molecule in the dilute phase. On the other hand, M.K. Purkait et al. [35] has already reported that in dilute phase, CMC of surfactant molecule decreases with increase in dye concentration at a fixed surfactant concentration.

4.7. Determination of change in Gibbs free energy (ΔG^{oo}) of CPE

The values of Gibbs free energy ($\Delta G°$) can be calculated from the enthalpy of solubilization ($\Delta H°$) and the entropy of solubilization ($\Delta S°$). Figs. 9(a)–(c) show the variations of Gibbs free energy change ($\Delta G°$) with temperature at a constant dye concentration and different surfactant concentrations. Change in Gibbs free energy ($\Delta G°$) values was negative for all the experiments. The negative values of $\Delta G°$ indicated that the dye solubilization is a spontaneous process and thermodynamically favorable. $\Delta G°$ increased linearly with temperature. For a constant dye concentration of 25 ppm and 0.01 M surfactant concentration, the negative value of $\Delta G°$ was 6,182.69 J mole^{-1} for 313.15 K, and it increased to 8,023.88 J mole^{-1} for 333.15 K. The increase in negative values of $\Delta G°$ with temperature implies the greater driving force for the solubilization of dye and is confirmed by the greater extent of dye extraction with increase in temperature [35]. On other hand, $\Delta G°$ decreased with increase in surfactant and dye concentrations. For a constant dye concentration of 25 ppm and a temperature of 333.15 K, the negative value of $\Delta G°$ was 8,023.88 J mole^{-1} for 0.01 M surfactant concentration, and it decreased to 5,139.02 J mole^{-1} for 0.04 M surfactant concentration. Table 4 presents the change of $\Delta G°$ with initial RTB G-133 concentrations. Table 4 and Fig. 8 represent that the value of $\Delta G°$ decreased with dye and surfactant concentrations at constant temperature in the micellar phase. Consequently, the amount of dye solubilization per mole of surfactant micelle decreased.

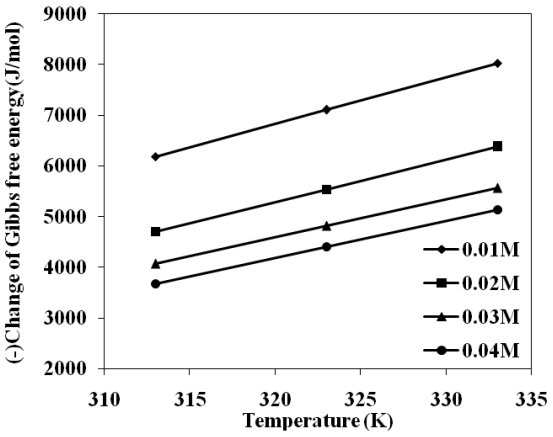

Fig. 9(a). Variation in Gibbs free energy change ($\Delta G°$) with temperature at 25 ppm RTB G-133 concentration and at different surfactant concentrations.

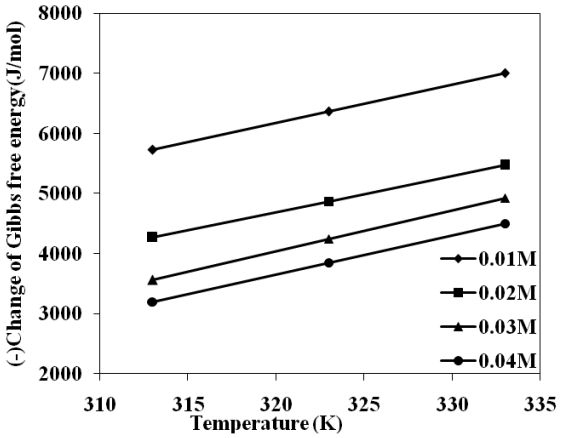

Fig. 9(b). Variation in Gibbs free energy change ($\Delta G°$) with temperature at 50 ppm RTB G-133 concentration and at different surfactant concentrations.

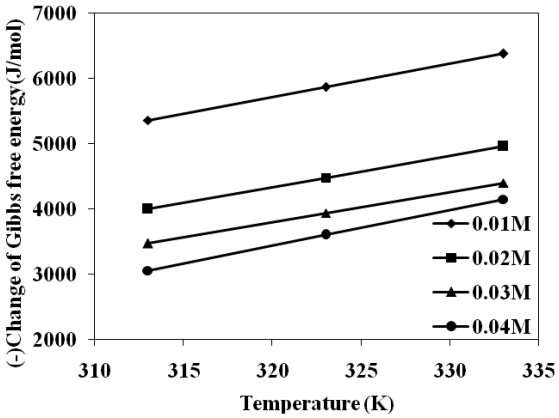

Fig. 9(c). Variation in Gibbs free energy change ($\Delta G°$) with temperature at 75 ppm RTB G-133 concentration and at different surfactant concentrations.

Table 4
Change in Gibbs free energy ($\Delta G°$) for CPE of RTB G-133 using TX-114 at different temperatures and concentrations of the dye and TX-100

TX-100 (moles L^{-})	RTB (ppm)	$-\Delta G°$ (J mol^{-1}) at temperature (K) × 10^{-3}		
		313.15 K	323.15 K	333.15 K
0.01	25	6,182.268	7,103.283	8,023.877
0.02	25	4,701.733	5,537.698	6,373.662
0.03	25	4,066.604	4,813.151	5,559.698
0.04	25	3,679.238	4,409.127	5,139.016
0.01	50	5,724.459	6,364.74	7,005.02
0.02	50	4,266.443	4,869.195	5,471.947
0.03	50	3,561.234	4,243.064	4,924.894
0.04	50	3,199.564	3,852.099	4,504.633
0.01	75	5,357.064	5,867.91	6,378.755
0.02	75	3,996.583	4,477.176	4,957.769
0.03	75	3,469.098	3,935.714	4,402.33
0.04	75	3,060.594	3,604.756	4,148.912

4.8. Solubilization isotherms

Isotherm data are fundamental requisites to design the CPE system. The dye solubilization potential of TX-114 at different temperatures can be determined from the experimental data, using the solubilization isotherms.

Figs. 10(a)–(c) depict the isotherms at various temperatures, for RTB G-133–TX-114 system. Most of the adsorption processes effectively employ the Langmuir type adsorption isotherms. Eq. (8) presents the expression of the Langmuir model:

$$q_e = \frac{mnC_e}{1+nC_e} \tag{8}$$

where q_e indicates the mole of dye solubilized per mole of surfactant. C_e represents the equilibrium concentration of the dye in dilute phase. m and n are the Langmuir constants denoting the capacity and energy of solubilization, respectively [8]. Values of m and n for each operating temperature are determined from experimental data using regression analysis. m and n vary with temperature and are fitted in a quadratic model as shown in Fig. 11(a)–(c). m and n values are expressed as a function of temperature as below:

For RTB G-133–TX-114 system at various concentrations of TX-114 (25, 50 and 75 ppm),

$$m = 0.013T^2 - 1.629T + 49.96 \quad (r^2 = 1) \tag{9}$$

$$n = -0.000T^2 + 0.015\mathrm{T} - 0.343 \quad (r^2 = 1) \tag{10}$$

$$m = -4\times10^{-5}\mathrm{T}^2 - 0.004T - 0.082 \quad (r^2 = 1) \tag{11}$$

$$n = 0.017T^2 - 2.222T + 73.74 \quad (r^2 = 1) \tag{12}$$

$$m = -0.358T^2 + 37.14T - 929.8 \ (r^2 = 1) \tag{13}$$

$$n = -8\times10^{-5}T^2 + 0.009T - 0.274 \quad (r^2 = 1) \tag{14}$$

where T is the temperature in degree Celsius.

At selected concentrations, DG^0 is positive and indicates the non-spontaneity of the adsorption and poor formation of stronger bonds between the adsorbent and adsorbate. Hence, the Langmuir's constant "m" is negative [37]. Moreover, at lower concentrations, it is found that the trend of the plot is similar to that of M.K. Purkait et al. [29], and at higher concentrations, it is observed that these models are less adequate to explain the complex adsorption process, since the constants represent surface binding energy and monolayer coverage.

4.9. Variation of fractional coacervate phase volume

It is necessary to study the variation of the fractional coacervate phase volume with the concentration of feed surfactant and the operating temperature to assess the performance of a CPE process. Hence, the fractional coacervate phase volume is related with the feed as follows:

$$F_c = aC_s^{\ b} \tag{15}$$

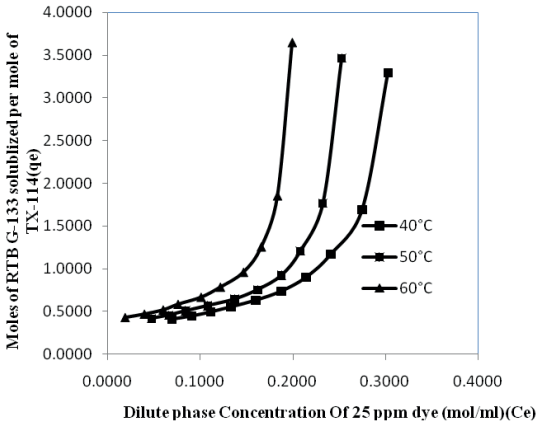

Fig. 10(a). Solubilization isotherm for 25 ppm RTB G-133 at various temperatures using TX-114.

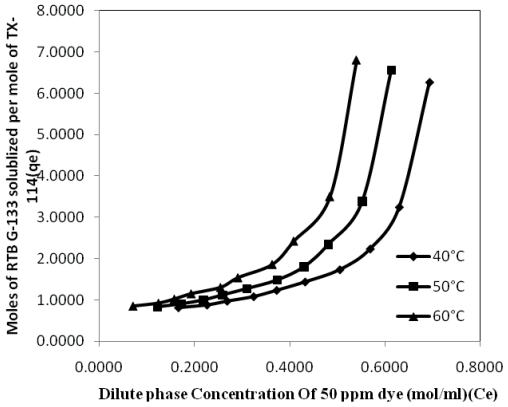

Fig. 10(b). Solubilization isotherm for 50 ppm RTB G-133 at various temperatures using TX-114.

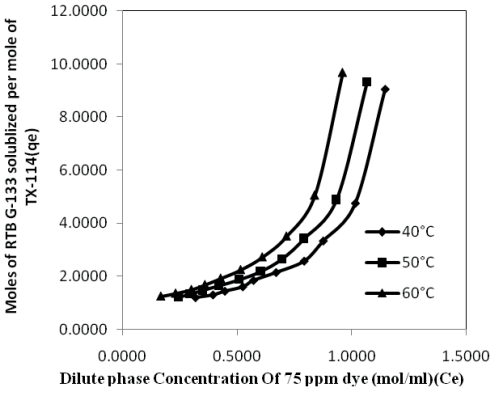

Fig. 10(c). Solubilization isotherm for 75 ppm RTB G-133 at various temperatures using TX-114.

where F_c refers to the fractional coacervate volume, and C_s indicates the molar concentration of the feed surfactant solution. It is aforementioned that a broad range of feed surfactant concentration and dye concentration is employed in the experiments at different operating temperatures. For fixed dye concentration, changes in the values of a and b with temperature are presented in Figs. 12(a)–(c) for RTB G-133. It is evident from Figs. 12(a)–(c) that a and b vary linearly with temperature and can be given as follows:

$$a = P + QT \tag{16}$$

$$b = R + ST \tag{17}$$

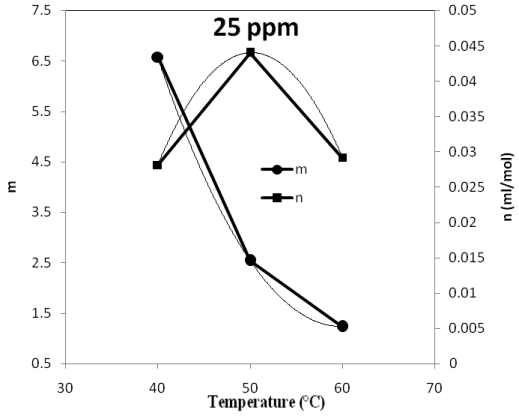

Fig. 11(a). Variation of the values of m and n with temperature for RTB G-133 in TX-114 of 25 ppm.

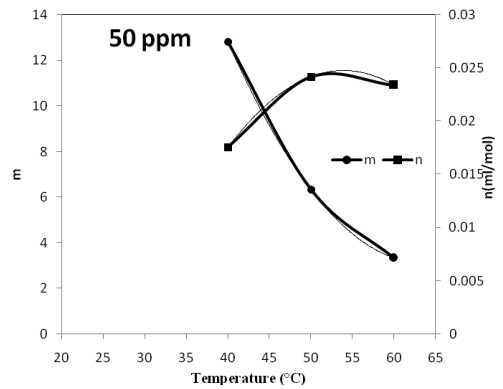

Fig. 11(b). Variation of the values of m and n with temperature for RTB G-133 in TX-114 of 50 ppm.

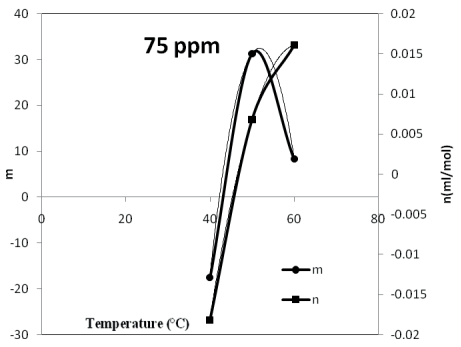

Fig. 11(c). Variation of the values of m and n with temperature for RTB G-133 in TX-114 of 75 ppm.

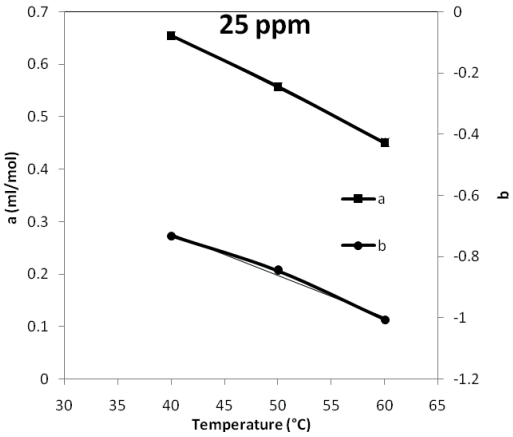

Fig. 12(a). Variation of the values of a and b with temperature for RTB G-133 (25 ppm) in TX-114.

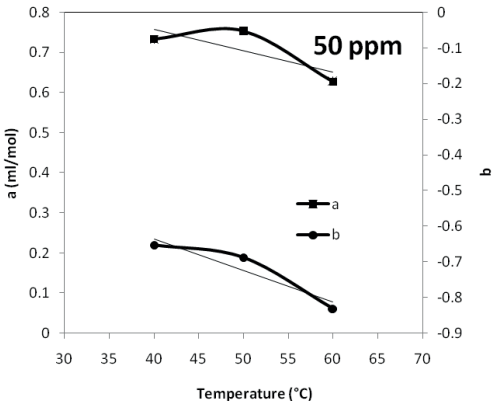

Fig. 12(b). Variation of the values of a and b with temperature for RTB G-133 (50 ppm) in TX-114.

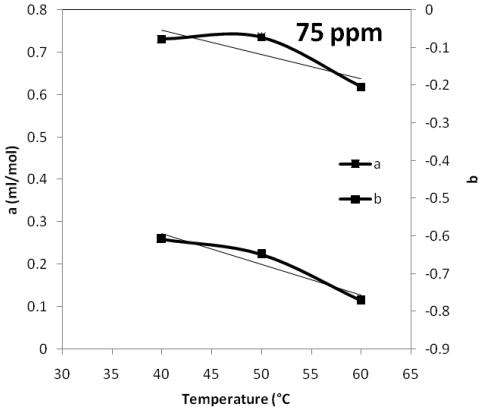

Fig. 12(c). Variation of the values of a and b with temperature for RTB G-133 (50 ppm) in TX-114.

The parameters *P*, *Q*, *R*, and *S* are determined for different dye concentrations. The value of *Q* ranges from –0.01 to –0.005, and *S* varies from –0.013 to –0.008. Characteristic changes in the values of the parameters *P* and *R* with respect to feed dye concentration are illustrated in Fig. 13.

A variation of *P* and *R* for RTB G-133 dye is given by the following correlation with the feed dye concentration:

$$P = 8\times10^{-5}C_0^{\,2} - 0.01C_0 + 1.262 \quad (r^2 = 1) \tag{18}$$

$$Q = 9\times10^{-5}C_0^{\,2} - 0.011C_0 + 0.041 \quad (r^2 = 1) \tag{19}$$

4.10. Determination of the surfactant needed for the removal of dye to a predetermined level without using salts

The amount of surfactant needed for removing dye up to a certain level is assessed by a procedure using the developed correlations (Eqs. (8)–(19)). The solubilization isotherm can be written as:

$$q_e = \frac{\text{Moles of dye solubilized}}{\text{Moles of RTB G}-133\text{ used}} = \frac{A}{X} \tag{20}$$

Moles of dye solubilized can be determined from mass balance:

$$A = V_0C_0 - V_dC_e \tag{21}$$

where V_0 and V_d are the volume of the feed and the dilute phase, respectively, after CPE. C_0 and C_e are the molar concentrations of feed dye and residual in the dilute phase after CPE. Therefore, C_e is the preferred concentration level of the dye for which CPE has to be executed. Eq. (21) can be expressed in terms of fractional coacervate phase volume (F_c) as follows:

$$A = V_0[C_0 - C_e(1-F_c)] \tag{22}$$

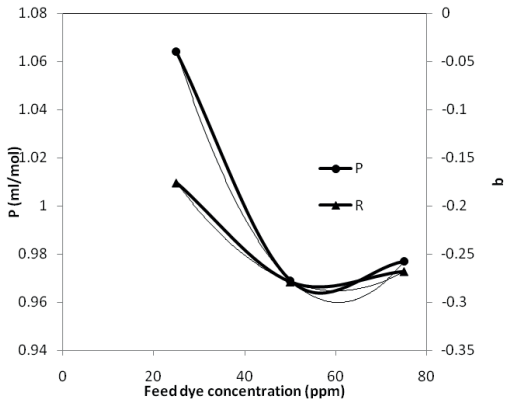

Fig. 13. Variation of the values of P and R with feed dye concentration for RTB G-133 in TX-114.

Using Eqs. (15), (20), and (22), the moles of surfactant required can be written as follows:

$$X = \frac{V_0}{q_e}[C_0 - C_e(1 - aC_s^{\,b})] \tag{23}$$

If C_s is the initial concentration of feed surfactant, *X* in Eq. (20) can be replaced as follows:

$$X = C_sV_0 \tag{24}$$

On equating Eqs. (23) and (24), the principal equation of C_s is derived as follows:

$$C_s = \frac{1}{q_e}[C_0 - C_e(1 - aC_s^{\,b})] \tag{25}$$

Writing q_e in terms of C_e from Eq. (8), C_s is expressed as follows:

$$C_s = \frac{(1+nC_e)[C_0 - C_e(1 - aC_s^{\,b})]}{mn\,C_e} \tag{26}$$

C_s can be calculated by trial and error from Eq. (26) if the values of feed dye concentration (C_0), preferred concentration of dye in the dilute phase (C_e), isotherm constants *m* and *n*, and design parameters are known. Eq. (26) was solved using typical temperature conditions, and the preferred concentration of dye in the dilute phase was fixed as 1.0 mg L^{-1} [29]. Thus, the concentration of surfactant needed for different concentrations of feed dye were assessed and plotted in Fig. 14 for RTB G-133 dye. It is evident from Fig. 14 that the concentration of surfactant required increases with the concentration of feed dye and is lowered at higher temperatures. Higher operating temperature demands higher energy input to the system. Hence, there prevails a trade-off between the dose of feed surfactant and the operating temperature with respect to concentration of feed dye to bring about a preferred level of dye removal.

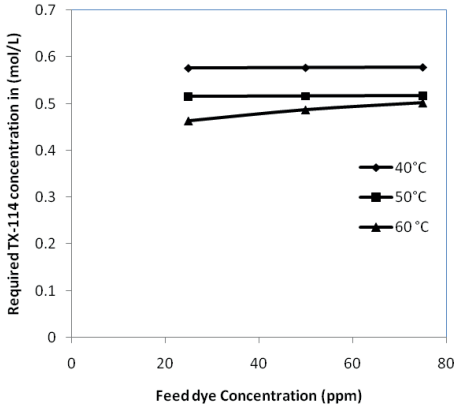

Fig. 14. Variation of required TX-114 concentration for different feed dye concentration at different temperatures with the desired dilute phase concentration of 1 ppm.

5. Conclusions

This paper reports the CPE of the dye RTBG-133 using TX-114 as non-ionic surfactant. All the experiments were performed in batch mode. The effects of surfactant and solute concentrations for different set of operating temperatures on CPE were investigated. Thermodynamic parameters such as change in Gibbs free energy ($\Delta G°$), change in enthalpy ($\Delta H°$), and change in entropy ($\Delta S°$) for CPE of TX-114–RTB G-133 dye system were also studied. Thermodynamic studies confirmed that the CPE is feasible and can be integrated in the textile or other dye processing industries for the treatment of colored effluents. The design proposed for CPE involves assessment of solubilization of RTBG-133 in surfactant and variation of fractional coacervate phase volume with operating conditions. The solubilization isotherms of RTB G-133 in TX-114 are defined by Langmuir type isotherm. The variations of the isotherm parameters with temperature are determined by the correlations developed. Fractional coacervate phase volume varies with feed surfactant concentration as aC_s^b. Parameters a and b vary linearly with temperature and $a = P + QT$ and $b = R + ST$. "a" decreases and "b" increases, respectively, with increase in temperature. Parameters P and R decrease with increase in feed dye concentration while Q and S remain almost constant. Therefore, in this regard, the concentration of surfactant needed to obtain 1 ppm of dye in dilute phase at a given temperature, and feed dye concentration is determined. At 60°C and for 25 ppm RTG B-133 feed concentration, 1 M surfactant is needed to achieve 1 ppm of remaining dye in the dilute phase. Moreover, low concentration of surfactant is required at higher temperatures.

Symbols

q_e	—	Moles of dye solubilized per mole of non-ionic surfactant
C_e	—	Equilibrium concentration of dye, moles L^{-1} before the completion of two phases
$\Delta G°$	—	Gibbs free energy
$\Delta S°$	—	Change in entropy
$\Delta H°$	—	Change in enthalpy
R	—	Gas constant
T	—	Temperature
A	—	Moles of dye solubilized in the micelles
V_0	—	Volume of the feed solution, ml
V_d	—	Volume of the dilute phase (ml) after CPE
F_c	—	Coacervate phase volume (ml) after CPE
C_0	—	Concentration of surfactant in feed solution
C_s	—	Molar concentration of the feed surfactant solution
m	—	Langmuir constants denoting the capacity of solubilization
n	—	Langmuir constants denoting the energy of solubilization
P, Q, R and S	—	Constants
a and b	—	Design parameters
X	—	Moles of surfactant

References

[1] G. Moussavi, R. Khosravi, The removal of cationic dyes from aqueous solutions by adsorption onto pistachio hull waste, Chem. Eng. Res. Des., 89 (2011) 2182–2189.

[2] P.K. Ray, Environmental pollution and cancer, J. Sci. Ind. Res., 45 (1986) 370–371.

[3] M.C. Silva, A.D. Corrêa, M.T.S.P. Amorim, P. Parpot, J.A. Torres, P.M.B. Chagas, Decolorization of the phthalocyanine dye reactive blue 21 by turnip peroxidase and assessment of its oxidation products, J. Mol. Catal., B Enzym., 77 (2012) 9–14.

[4] J.R. Aspland, Reactive dyes and their application, Tex. Chem. Color., 24 (1992) 31–36.

[5] A. Dursun, O. Tepe, G. Dursun, Use of carbonised beet pulp carbon for removal of Remazol Turquoise Blue-G 133 from aqueous solution, Environ. Sci. Pollut. Res., 20 (2013) 431–442.

[6] A.A. Vaigan, M.R.A. Moghaddam, H. Hashemi, Effect of dye concentration on sequencing batch reactor performance, Iranian J. Environ. Health Sci. Eng., 6 (2009) 11–16.

[7] S. Chakraborty, M.K. Purkait, S. DasGupta, S. De, J.K. Basu, Nanofiltration of textile plant effluent for color removal and reduction in COD, Sep. Purif. Technol., 31 (2003) 141–151.

[8] C. Namasivayam, D. Kavitha, Removal of Congo Red from water by adsorption onto activated carbon prepared from coir pith, an agricultural solid waste, Dyes Pigm., 54 (2002) 47–58.

[9] M.K. Purkait, S. DasGupta, S. De, Removal of dye from wastewater using micellar-enhanced ultrafiltration and recovery of surfactant, Sep. Purif. Technol., 37 (2004) 81–92.

[10] I. Arvanitoyannis, I. Eleftheriadis, E. Tsatsaroni, Influence of pH on adsorption of dye-containing effluents with different bentonites, Chemosphere, 18 (1989) 1707–1711.

[11] S.H. Lin, C.M. Lin, Treatment of textile waste effluents by ozonation and chemical coagulation, Water Res., 27 (1993) 1743–1748.

[12] A. Majcen-Le Marechal, Y.M. Slokar, T. Taufer, Decoloration of chlorotriazine reactive azo dyes with H_2O_2/UV, Dyes Pigm., 33 (1997) 281–298.

[13] M. Neamtu, A. Yediler, I. Siminiceanu, M. Macoveanu, A. Kettrup, Decolorization of disperse red 354 azo dye in water by several oxidation processes—a comparative study, Dyes Pigm., 60 (2004) 61–68.

[14] N. Kannan, M.M. Sundaram, Kinetics and mechanism of removal of methylene blue by adsorption on various carbons—a comparative study, Dyes Pigm., 51 (2001) 25–40.

[15] J.H. Bae, D.I. Song, Y.W. Jeon, Adsorption of anionic dye and surfactant from water onto organomontmorillonite, Sep. Sci. Technol., 35 (2000) 353–365.

[16] A.K. Golder, N. Hridaya, A.N. Samanta, S. Ray, Electrocoagulation of methylene blue and eosin yellowish using mild steel electrodes, J. Hazard. Mater., 127 (2005) 134–140.

[17] N.D. Gullickson, J.F. Scamehorn, J.H. Harwell, Liquid-Coacervate Extraction, J.F. Scamehorn, J.H. Harwell (Eds.), Surfactant-Based Separation Processes, Marcel Dekker Inc, New York, 1989, pp. 139–152.

[18] W. Kimchuwanit, S. Osuwan, J.F. Scamehorn, J.H. Harwell, K.J. Haller, Use of a micellar-rich coacervate phase to extract trichloroethylene from water, Sep. Sci. Technol., 35 (2000) 1991–2002.

[19] R. Pool, P.G. Bolhuis, The influence of micelle formation on the stability of colloid surfactant mixtures, Phys. Chem. Chem. Phys., 12 (2010) 14789–14797.

[20] Md.S. Alam, A.B. Mandal, Thermodynamic studies on mixed micellization of amphiphilic drug amitriptyline hydrochloride and nonionic surfactant Triton X-100, J. Mol. Liq., 168 (2012) 75–79.

[21] Md.S. Alam, V. Nareshkumar, N. Vijayakumar, K. Madhavan, A.B. Mandal, Effect of additives on the CP of mixed surfactant (non-ionic Triton X-114 + cationic gemini 16-6-16) solutions, J. Mol. Liq., 194 (2014) 206–211.

[22] Md.S. Alam, A.M. Siddiq, N. Kamely, M. Priyadharshini, V. Mythili, A.B. Mandal, Influence of the additives on clouding of non-ionic surfactant Triton X-114 solutions: evaluation of thermodynamics at the CP, J. Dispersion Sci. Technol., 36 (2015) 1569–1576.

[23] Md.S. Alam, A.B. Mandal, The clouding phenomena of mixed surfactant (non-ionic Triton X-114 + cationic gemini 16-5-16) solutions: influence of inorganic and organic additives on the cloud point, J. Mol. Liq., 212 (2015) 237–244.

[24] C.D. Stalikas, Micelle-mediated extraction as a tool for separation and preconcentration in metal analysis, TrAC, Trends Anal. Chem., 21 (2002) 343–355.
[25] M.K. Purkait, S.S. Vijay, S. DasGupta, S. De, Separation of congo red by surfactant mediated cloud point extraction, Dyes Pigm., 63 (2004) 151–159.
[26] A. Appusamy, I. John, K. Ponnusamy, A. Ramalingam, Removal of crystal violet dye from aqueous solution using triton X-114 surfactant via cloud point extraction, Eng. Sci. Technol., Int. J., 17 (2014) 137–144.
[27] A. Arunagiri, P. Kalaichelvi, S. Cherukuria, A. Vijayan, Studies on removal of reactive blue dye using cloud point extraction, Int. J. Chem. Environ. Eng., 3 (2012) 16–23.
[28] R. Joarder, D. Santra, S. Marjit, M. Sarkar, Preconcentration and recovery of pesticides from soil and water by dispersive liquid-liquid extraction, Eur. Chem. Bull., 3 (2014) 612–616.
[29] M.K. Purkait, S. Banerjee, S. Mewara, S. DasGupta, S. De, Cloud point extraction of toxic eosin dye using Triton X-100 as nonionic surfactant, Water Res., 39 (2005) 3885–3890.
[30] M.K. Purkait, S. DasGupta, S. De, Performance of TX-100 and TX-114 for the separation of chrysoidine dye using cloud point extraction, J. Hazard. Mater., 137 (2006) 827–835.
[31] F.H. Quina, W.L. Hinze, Surfactant-mediated cloud point extractions: an environmentally benign alternative separation approach, Ind. Eng. Chem. Res., 38 (1999) 4150–4168.
[32] R. Carabias-Martínez, E. Rodríguez-Gonzalo, B. Moreno-Cordero, J.L. Pérez-Pavón, C. García-Pinto, E. Fernández Laespada, Surfactant cloud point extraction and preconcentration of organic compounds prior to chromatography and capillary electrophoresis, J. Chromatogr. A, 902 (2000) 251–265.
[33] A. Appusamy, P. Purushothaman, K. Ponnusamy, A. Ramalingam, Separation of methylene blue dye from aqueous solution using Triton X-114 surfactant, J. Thermodyn., 2014 (2014) 1–16.
[34] J.-L. Li, B.-H. Chen, Equilibrium partition of polycyclic aromatic hydrocarbons in a cloud-point extraction process, J. Colloid Interface Sci., 263 (2003) 625–632.
[35] M.K. Purkait, S. DasGupta, S. De, Determination of thermodynamic parameters for the cloud point extraction of different dyes using TX-100 and TX-114, Desalination, 244 (2009) 130–138.
[36] M.K. Purkait, S. DasGupta, S. De, Determination of design parameters for the cloud point extraction of congo red and eosin dyes using TX-100, Sep. Purif. Technol., 51 (2006) 137–142.
[37] A.A. Kale, Evaluation of sieved biomass of *Cicer arientinum* (horse bean) for removal of methylene blue: batch study, Int. J. Recycl. Org. Waste Agric., 2:18 (2013) 1–8.